Tetrahedron 64 (2008) 10258–10266

Contents lists available at ScienceDirect

Tetrahedron

journal homepage: www.elsevier.com/locate/tet

Resorcinarene-dendrimers with stilbene moieties for optoelectronics

Irina V. Lijanova [a], Ivana Moggio [b], Eduardo Arias [b], Tatiana Klimova [c], Marcos Martínez-García [a,*]

[a] Instituto de Química, UNAM, Cd. Universitaria, Circuito Exterior, Coyoacán, C.P. 04510, México D.F., Mexico
[b] Centro de Investigación en Química Aplicada (CIQA), Boulevard Enrique Reyna 140, C.P. 25253, Saltillo, Mexico
[c] Facultad de Química, UNAM, Cd. Universitaria, Circuito Interior, Coyoacán, C.P. 04510, México D.F., Mexico

ARTICLE INFO

Article history:
Received 28 July 2008
Accepted 1 August 2008
Available online 9 August 2008

Keywords:
OPV
Resorcinarene
Dendrimers
Cyclic voltammetry
Electrochromism

ABSTRACT

Dendrimers with resorcinarene core and π-conjugated dendron branches with 16 and 32 stilbene groups have been synthesized and characterized by ^{1}H and ^{13}C NMR, FTIR, UV–vis, fluorescence spectroscopy, MALDI-TOF, electrospray or FAB^{+} mass spectrometry, and elemental analysis. Homogeneous thin films of resorcinarene-dendrimers deposited on quartz, glass or ITO substrates were prepared by spin-coating. All the materials showed absorption in the UV region in both chloroform solutions and thin films. The band gap energies (E_g) determined from both UV–vis spectroscopy and voltammetry were in the semiconducting range. A slight decrease in the E_g values was observed when passing from the first generation of dendrimers to the second one, which can be attributed to an increase in the π-conjugated system. The fluorescence quantum yield of the molecules in solution was low and practically null in the solid state. Nevertheless, a very interesting behavior was observed in the reductive voltammetric cycle, where electrochromism from transparent to blue forms occurred in the film by n-doping process; property that makes these materials suitable for the development of electrochromic devices such as smart windows.

1. Introduction

In the development of novel conjugated systems for optoelectronics, poly(*p*-phenylenevinylene) (PPV) and its oligomers have attracted much attention since 1990s because of their excellent electroluminescent and electroconductive properties[1,2] and the possibility to develop light emitting diodes, electrochemical cells, solar cells, etc. Recently, a new technology called 'Smart Windows' has emerged as an alternative to optimize the solar energy by controlling the amount of daylight and heat gain through the windows of buildings, airplanes, and vehicles.[3] A smart window is a glass (or switchable glass) that can change its light transmission property from transparent to opaque or colored when an electrical potential is applied. The active material in smart windows has electrochromic properties such as those exhibited by some liquid crystals or dies, and also by some conjugated polymers that can pass through different redox forms.[4] Since that all π-conjugated macromolecules are potentially electrochromic due to the injection of charge carriers that change their electronic structure resulting in a shift of their optical absorption, π-conjugated dendrimers are ideal model materials to ascertain a proper structure–property relationship because of their monodispersity, their well-defined size, shape, and the possibility to be modified with functional end groups[9] to give rise to nanoarchitectures that can be built-up through self-assembly.[5–8] At this respect, an exciting number of functional assemblies that exploit unique dendritic properties have been reported.[10–15] Recently, we have reported that dendrimers containing an oligo(phenylenevinylene) or resorcinarene core decorated with linear and branching π-conjugated dendrons containing phenyl groups present interesting optical properties.[16] Here, we report the synthesis and the optical and electrochemical properties of the first and second generation of dendrimers with π-conjugated branches and resorcinarene core.

2. Results and discussion

2.1. Synthesis and chemical characterization of dendrons and dendrimers

Dendrons of first and second generation containing styryl groups were prepared using the Heck reaction. Styrene **1** or 1,3-di(*E*)-styryl-5-vinylbenzene **6** was coupled with 3,5-dibromobenzaldehyde **2** in dimethyl formamide–triethylamine (5:1) using palladium acetate as catalyst (Scheme 1). Both compounds **3** and **7** were obtained in 60% and 70% yields, respectively. They have *E*-configuration as it was evidenced by the high value (ca. 16 Hz) of the coupling constant for the AB system of the vinylic protons. Aldehydes **3** and **7** were reduced with $LiAlH_4$ in THF to give alcohols **4** and **8** in 90% yield, which were converted into chlorides **5** and **9** upon treatment with thionyl chloride and pyridine in dichloromethane. Dendrons **5**[14] and **9** are

* Corresponding author.
E-mail address: margar@servidor.unam.mx (M. Martínez-García).

0040-4020/$ – see front matter
doi:10.1016/j.tet.2008.08.007

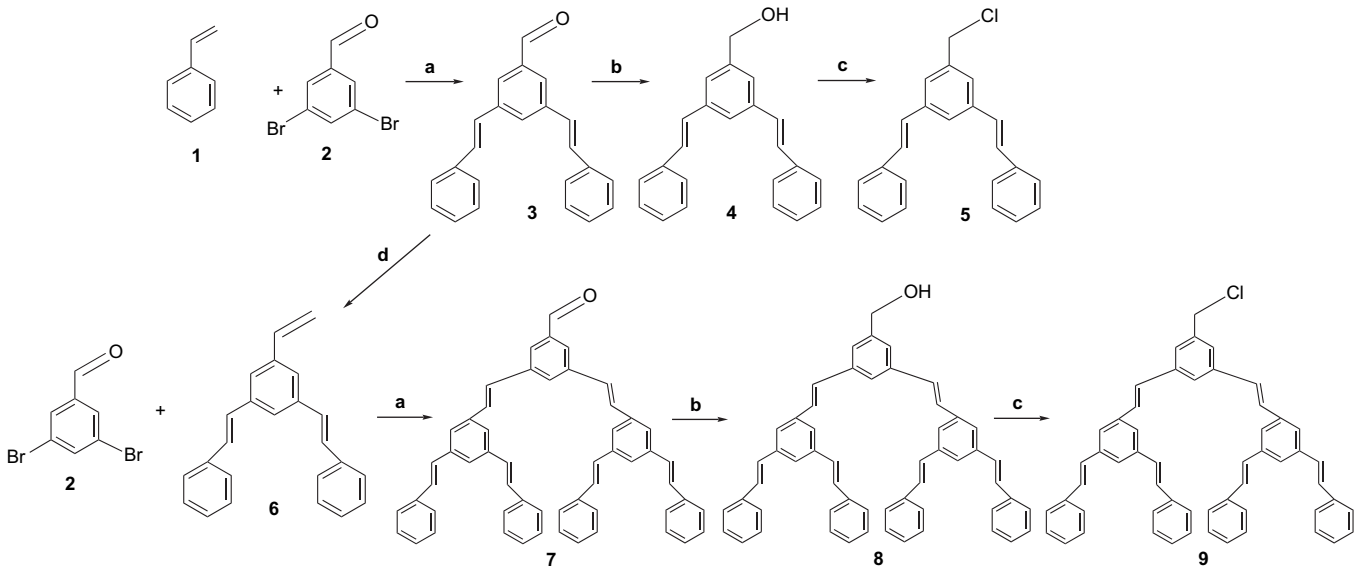

Scheme 1. Synthesis of dendrons of first and second generations: (a) $Pd(OAc)_2$, TOP, DMF–Et_3N, 120 °C; (b) THF, $LiAlH_4$, 0 °C; (c) Py, CH_2Cl_2, $SOCl_2$, 0 °C; (d) $CH_3(Ph)_3PBr$, *n*-BuLi, THF, 0 °C.

the first and second generation dendrons of the stilbene families (Scheme 1).

Resorcinarenes **13**–**15** (Scheme 2) were obtained from resorcinol and three aldehydes (hidrocinnamaldehyde **10**, hexanal **11**, and dodecanal **12**). The products were obtained as precipitates. The structure of these resorcinarenes was confirmed by NMR and FAB^+ mass spectrometry. Cyclic tetramers gave a well resolved triplet at 4.36 ppm, which is attributed to methine protons with an *rccc* conformation.[10]

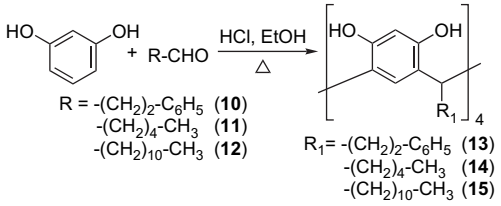

Scheme 2. Synthesis of resorcinarenes **13**, **14**, and **15**.

The synthesis of functionalized dendrimers **16**–**21** involves O-alkylation of dendron **5** or **9** with resorcinarenes **13**–**15** (Scheme 3). The reaction was carried out in acetone and K_2CO_3 at reflux for 7 days and the dendrimers were obtained in good yields.

2.2. Optical properties

The optical properties of the resorcinarene-dendrimers were studied by the UV–vis spectra of resorcinarene-dendrimers **16**–**21** in chloroform together with those of the dendron precursors **5** and **9** are shown in Figure 1 and summarized in Table 1.

All of the molecules absorb in the UV region. The first generation dendrimers exhibit a peak at 302 nm due to the p–p electronic transitions of the OPV moieties. This band is red-shifted to 315 nm in the spectra of dendrimers of the second generation due to the presence of more phenyl rings in the dendron branches increasing an extension of the p-conjugation. However, because of the *meta*-substitution, the increase in the effective conjugation is modest and the bathochromic shift from the first to the second generation is of just 13 nm. When comparing the spectra with those of the corresponding dendron precursors, difference in both shape and intensity can be observed even if the wavelength of the peaks remained unchanged. The resorcinarene spectra present a blurring that could be indicative of intramolecular interchromophore interactions according to the data reported by Armaroli and Nierengarten et al. for OPV calix[4]arenes.[17,18] The fluorescence spectra are reported in Figure 2.

Similarly to what is observed for the absorption spectra, the emission maxima is at 387 nm for the first generation and at 391 nm for the second generation, because of the increase in the π-conjugated chain length. The increase in the dendron generation has an effect on the shape of the fluorescence spectra. In fact, the first generation family exhibits only a broad band, while the spectra of the second generation present an intense band with an extra peak that could be likely ascribed to vibronic coupling. Other possible explanations are, however, to be taken in to account: first of all, the OPV dendrons are substituted in a resorcinarene structure that can assume different conformations due to the methine bridge. This could give rise to different excited states. The second layer of the second generation dendrimer is likely different electronically than the inner layer. As a result, the extra peak could also be due to the emission from two different chromophores that overlap in the absorption spectra or to partial energy transfer from one chromophore to the other as observed by Moore on a phenylene ethynylene energy gradient dendrimer.[19] The quantum yield is very low for all of the molecules, with an apparent slight improvement for the second generation in agreement with the modest increase in the conjugation or the possible energy transfer. However, considering the error estimated in the literature for its determination, we can conclude that all of the molecules present a quantum yield in solution lower than 10%. This result is a bit surprising considering that for OPV derivatives, inclusive OPV calix[4]arenes and bi(phenylene vinylidenes),[20] high values for the fluorescence quantum yields are usually found. At this respect, it is important to remark that photophysical studies are necessary to clearly explain the reason for these results. In fact the photophysics of phenylene vinylene polymers is complex and reason of strong debate.[2] On the basis of the optical data so far obtained and the literature works, we can hypothesize that: (i) the *meta*-substitution of the stryryls dendrons, (ii) their dynamic cis–trans conformation, and (iii) their substitution in the resorcinarene structure can lead to substantial intramolecular quenching. It is well known that the *meta*-

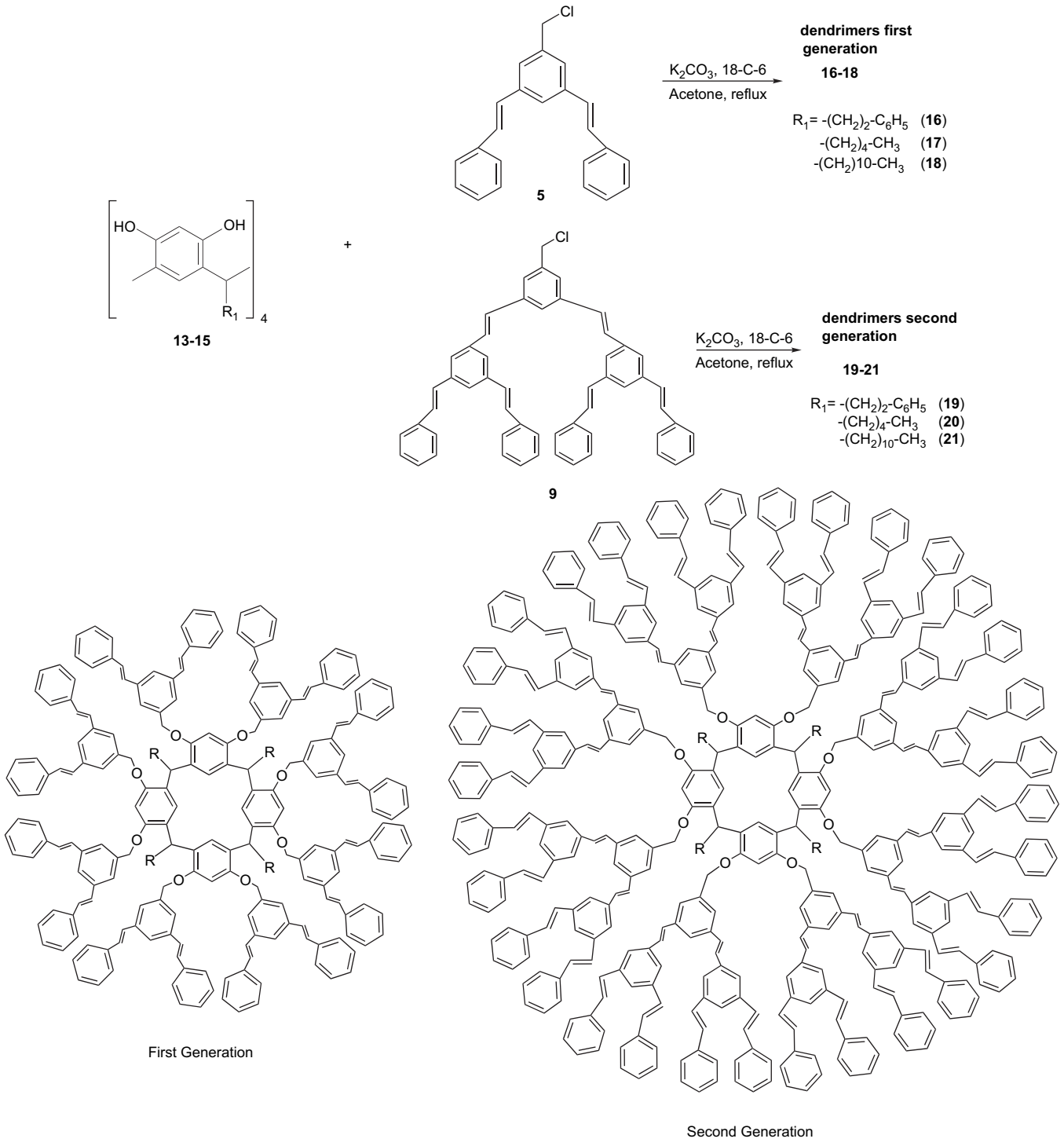

Scheme 3. Synthesis and chemical structures of the resorcinarene-dendrimers.

substitution decreases conjugation. Moreover, Armaroli and Nierengarten report partial electronic deconjugation among OPV branches when assembled into the calix[4]arenes that lowers the quantum yield with respect to a corresponding model compound.[17] As a final remark, both the UV–vis and fluorescence spectra of resorcinarene-dendrimers in solution do not change notably within each family indicating that there is no effect of the spacers between two adjacent OPV branches in the molecule, in agreement with the results previously reported on other conjugated resorcinarene-dendrimers.[16]

Thin films were prepared by spin-coating technique using chloroform solutions of the dendrimers **16**–**21**. The morphology is of granular type, i.e., consisting of a flat surface that coexists with grains. Similar behavior was observed for instance in a crown ether containing PPV.[21] In Figure 3, a bidimensional tapping AFM image for a sample of **21** is shown as example. According to particle analysis, the grains have an apparent 85 nm of average size and 9 nm of height. When corrected for the ratio of curvature of the tip, the average diameter decreases to around 70 nm. Unfortunately, the molecule length on its extended conformation was

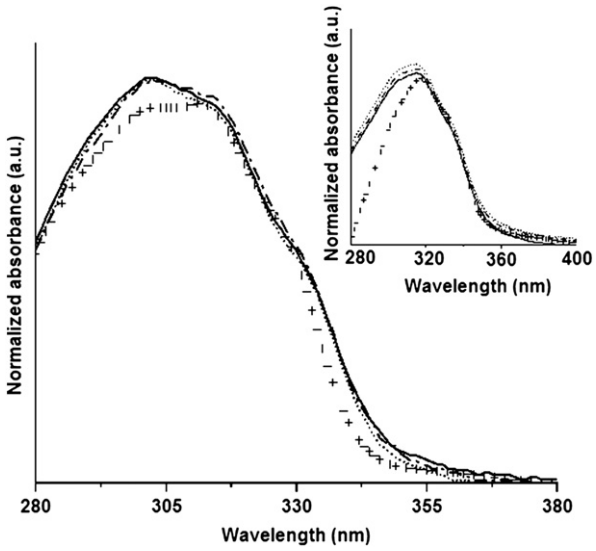

Figure 1. UV–vis spectra of first generation resorcinarene-dendrimers in chloroform: **16** (solid line), **17** (dashed line), **18** (dotted line), and precursor dendron **5** (crosses). Inset: corresponding spectra for the second generation resorcinarene-dendrimers in chloroform: **19** (thick solid line), **20** (thick dashed line), **21** (thick dotted line), and precursor dendron **9** (crosses).

Table 1
Optical properties of resorcinarene-dendrimers in chloroform solutions

Dendrimer	$\lambda_{max\ abs}$ (nm)	ε (L/g/cm)	$\lambda_{max\ emis}$ (nm)	ϕ (%)
16	302	114.3	387	5.1
17	302	65.0	387	5.0
18	302	99.4	387	6.3
19	315	97.5	391	10.7
20	315	103.1	391	12.2
21	315	119.4	391	7.5

not possible to determine by molecular simulation (using the program Spartan's 04) due to the large number of atoms that impeded to obtain the minimal energy conformation, however, the resorcinarene-dendrimers' size is likely lower than the grain size suggesting that they rather correspond to agglomerates. The presence of agglomerates is typical of conjugated macromolecular

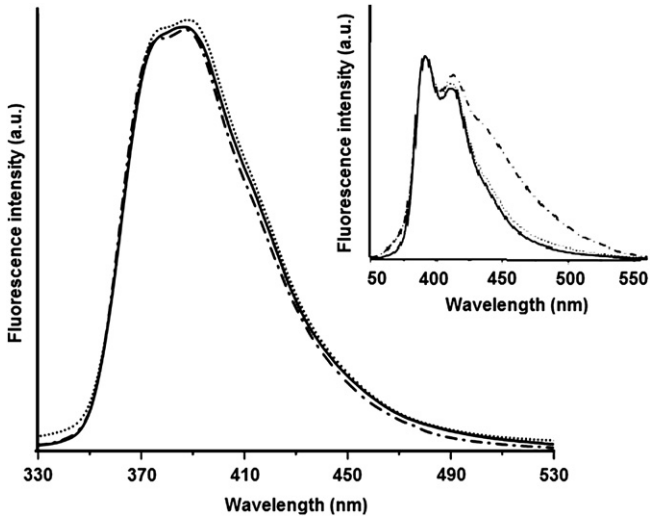

Figure 2. Fluorescence spectra of first generation resorcinarene-dendrimers: **16** (solid line), **17** (dashed line), and **18** (dotted line) in chloroform. Inset: corresponding spectra for the second generation resorcinarene-dendrimers in chloroform: **19** (thick solid line), **20** (thick dashed line), and **21** (thick dotted line).

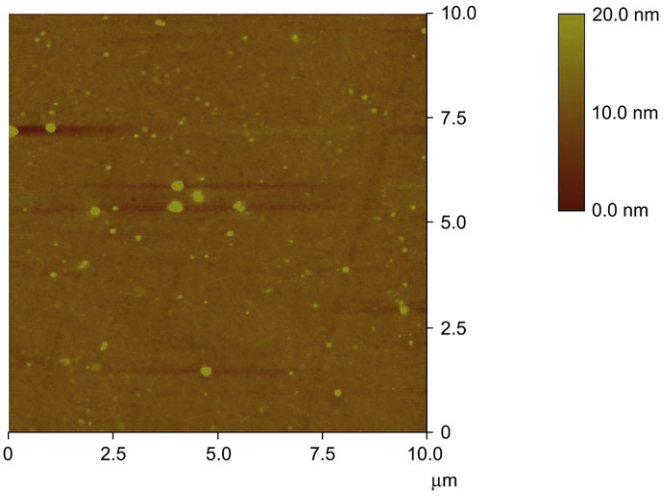

Figure 3. Tapping mode AFM bidimensional image of a thin film of **21** prepared by spin-coating.

films as the strong p–p interactions promote intra and intermolecular packing. Despite of this, the root mean square roughness is low (Rq=1.920 nm) indicating that the surface is quite smooth. The corresponding optical properties are collected in Table 2.

The UV–vis and fluorescence spectra of the films are shown in Figure 4a (dendrimers of first generation) and b (dendrimers of second generation). The absorption maxima are similar to those in solution suggesting that the intermolecular interactions in the films are similar to those in chloroform. The fluorescence maxima were observed at 391–393 nm for the first generation dendrimers **16** and **18** and at 418–419 nm for the second generation dendrimers **19**–**21**. The quantum yield is extremely low and could not be determined for **17** due to the very noisy signal detected in the fluorescence spectrum for a film having ca. 100 nm of thickness. This result, as a whole, is not very surprising considering that electronic effects in solid state usually decrease the emission quantum yield when compared to the solutions, where the molecules are isolated. In our case, these resorcinarenes present a very low quantum yield even in solution; therefore, it is reasonable to obtain also lower values in films. It is to point out that the quantum yield in thin films was indirectly obtained as is explained in Section 4. The direct measurement by the integrating sphere method was not possible because determination of the quantum yield for high refractive samples on films is difficult due to the fact that they present angular dependence. Thus, the determination of this parameter by a modified secondary method introduces a higher error than if it were directly measured by the integrating sphere. The η values thus are intended to give an estimation of the fluorescent properties of the materials in order to visualize their possible performance in LED application. At this respect, the present molecules do not appear as appealing materials for electroluminescent devices. The optical band gap corresponds to semiconducting materials with a lower value for the second

Table 2
Optical properties of resorcinarene-dendrimers in thin films

Dendrimer	$\lambda_{max\ abs}$ (nm)	ε (nm^{-1}) 10^{-3}	E_g (eV)	$\lambda_{max\ emis}$ (nm)	η (%)
16	302	7.98	3.48	393	2.5
17	300	7.68	3.47	ND	ND
18	301	8.87	3.45	391	4.0
19	310	8.92	3.28	419	3.2
20	315	7.20	3.26	418	1.8
21	312	11.08	3.29	418	0.9

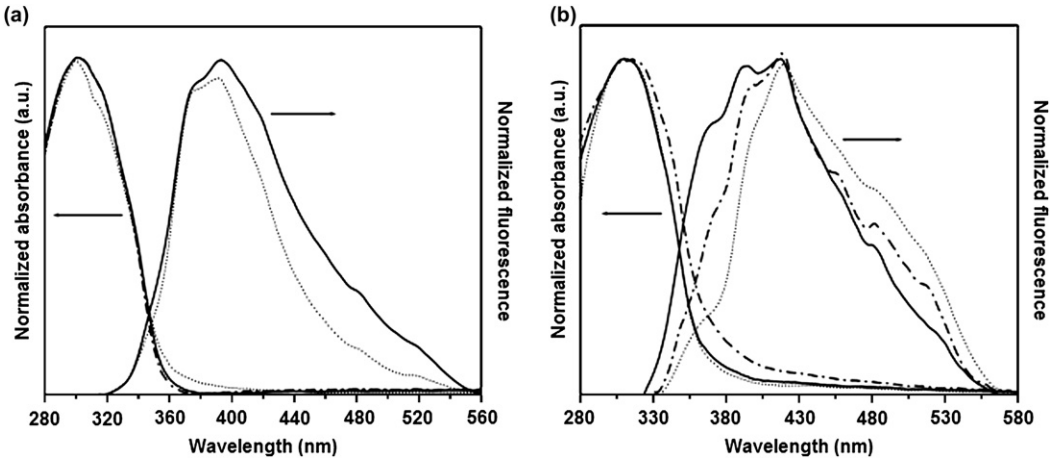

Figure 4. (a) UV–vis and fluorescence spectra of spun films (approximately 100 nm thickness) of **16** (solid line), **17** (dash-dotted line), and **18** (dotted line). (b) UV–vis and fluorescence spectra of spun films (approximately 100 nm thickness) of **19** (solid line), **20** (dash-dotted line), and **21** (dotted line).

generation molecules in agreement with their slightly higher electronic delocalization.

Figure 5a and b shows the corresponding oxidative–reductive voltagramms from cyclic voltammetry obtained on thin films of the second generation dendrimers **19**, **20**, and **21**, as the most representative electrochemical curves. An interesting feature observed for both generations of dendrimers studied is that at the beginning of the reduction (E_{red} onset), films developed a slightly sky blue color that intensifies to deep blue when the maximum reduction is reached (E_{red} max). The image is inserted in the Figure 5b for **21** at −2.28 mV. It should also be pointed out that only the second generation dendrimers show a well-defined reduction in the voltagramms. For the first generation molecules' potential values E_{red} onset and E_{red} max were assigned in accordance with the color change development of the films. A film of **21** was retired when the maximal reduction (blue film) and oxidation (bleach film) process was reached and the UV–vis spectrum (Fig. 6) revealed the appearance of a very broad band at 546 nm that does not exhibit any increase in intensity as a function of the applying potential. This result suggests that both p- and n-doping process is carried out in the Bu_4NPF_6–CAN electrolyte solution at ca. 1.63 V, and −2.28 V, respectively, and in agreement with other π-conjugated molecules reported in the literature.[22] In addition, a red shift of the p–p electronic transitions from 312 nm (neutral form, curve a) to 319 nm (p-doped film, curve b) and to 326 nm (n-doped film, curve c) is observed, showing that electron delocalization increases during both processes, presumably because the styryl moieties assume a more quinoide structure as a consequence of doping as usually found for conjugated polymers with not equivalent electronic ground states. From these experiments, we therefore obtain three band gaps either for the oxidation or reduction processes at the onset, at the maxima, and at the midpoint; all the electrochemical parameters are reported in Table 3. From this table it can be seen that: (i) E_g in the midpoint shows no differences by changing the length and type of the substituents in the methine bridges in agreement with the theory that s electrons are not involved in the redox process, (ii) there is a minimal difference in the band gap between those of the first generation **16**–**18** E_g=3.51±0.07 eV with that found for those of the second generation **19**–**21** E_g=3.36±0.02 eV, suggesting that p electrons delocalization along the styryls length is minimal, (iii) it is interesting to observe that the optical band gap (Table 2) matches well with the electrochemical band gap in the midpoint, and (iv) materials can be classified as semiconductors. Considering that the thin films of these resorcinarene-dendrimers are transparent, not fluorescent, and that the materials show semiconducting properties and exhibit electrochromism, further investigation into their application in smart windows is warranted.

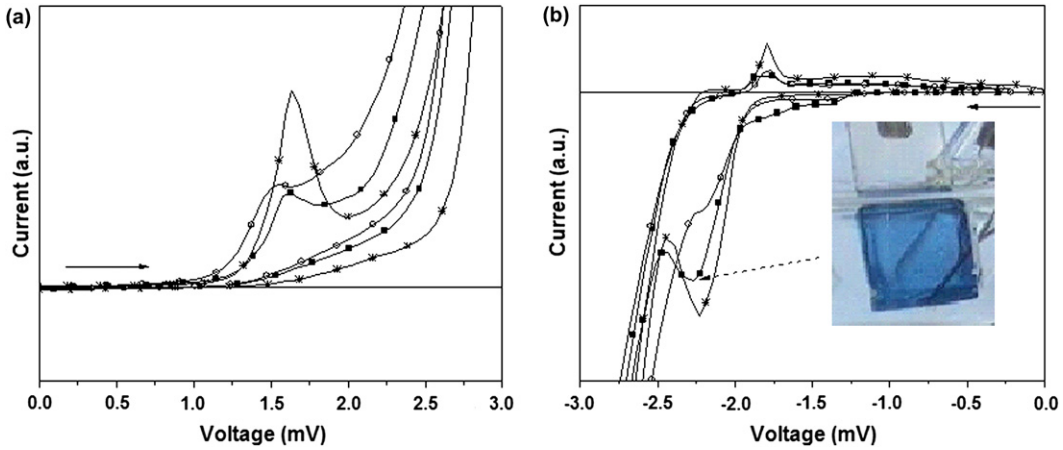

Figure 5. Cyclic voltagramms of the (a) oxidative and (b) reductive cycles for the second generation dendrimers **19** (○), **20** (*), and **21** (■) deposited on glass coated ITO. The inset image shows the blue form of **21** at the maximal reduction process.

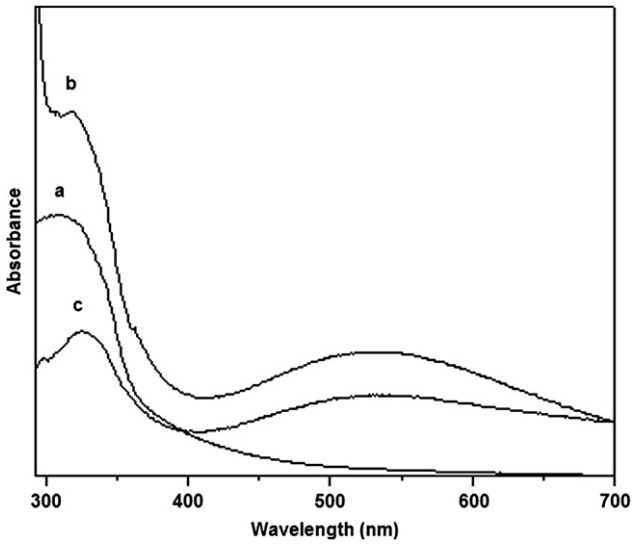

Figure 6. UV–vis spectra for the second generation dendrimer **21** recorded: (a) in its neutral form, (b) at its maximal oxidation peak (1.63 V), and (c) at its maximal reduction peak (−2.28 V).

Table 3
Electrochemical properties of thin films of the resorcinarene-dendrimers coated on ITO as the working electrode at scan rates of 50 mV/s versus $Fe–Fe^{+}$

Molecule	**16**	**17**	**18**	**19**	**20**	**21**
E_{ox} onset (V)	1.023	1.085	1.162	1.043	1.096	1.072
E_{ox} max (V)	1.625	1.669	1.802	1.548	1.576	1.634
E_{red} onset (V)	−1.867	−1.819	−1.843	−1.845	−1.815	−1.837
E_{red} max (V)	−2.417	−2.409	−2.495	−2.259	−2.266	−2.228
LUMO onset (eV)	−2.933	−2.981	−2.957	−2.955	−2.985	−2.963
LUMO max (eV)	−2.383	−2.391	−2.305	−2.541	−2.534	−2.572
HOMO onset (eV)	−5.823	−5.885	−5.862	−5.843	−5.896	−5.872
HOMO max (eV)	−6.425	−6.469	−6.602	−6.348	−6.376	−6.434
E_g onset	2.890	2.904	2.905	2.888	2.911	2.909
E_g max	4.042	4.078	4.297	3.807	3.842	3.862
Band gap (E_g) midpoint	3.466	3.491	3.601	3.347	3.376	3.385

3. Conclusions

Resorcinarene-dendrimers with 16 and 32 stilbene groups attached to resorcinarene core were synthesized. All of the resorcinarene-dendrimers absorb in the UV region in both chloroform solution and thin films. The change from the dendrimers of first generation to those of the second generation resulted in a slight decrease in the band gap energy (E_g). The fluorescence quantum yield of the molecules in solution is low and practically null in the solid state. Nevertheless, a very interesting behavior is observed in the reductive voltammetric cycle, where electrochromism from transparent (neutral form) to blue (reduced form) occurs in the film; property that makes these materials suitable for the development of electrochromic devices such as smart windows.

4. Experimental section

4.1. Materials, equipments, and methods

Solvents and reagents were purchased as reagent grade and used without further purification. Acetonitrile (AC) was first passed by a plug of silica gel and then distilled from CaH_2. Acetone was distilled over calcium chloride. Tetrahydrofuran was distilled from sodium and benzophenone. Column chromatography was performed on Merck silica gel 60 Å (70–230 mesh). ^{1}H and ^{13}C NMR were recorded on a Varian-Unity-300 MHz with tetramethylsilane (TMS) as an internal reference. Infrared (IR) spectra were measured on a spectrophotometer Nicolet FT-SSX. Elemental analysis was determined by Galbraith Laboratories, INC Knoxville. FAB^{+} mass spectra were taken on a JEOL JMS AX505 HA instrument. Electrospray mass spectra were taken on a Bruker Daltonic, Esquire 6000. The UV–vis absorption spectra were obtained with a Shimadzu 2401 PC spectrophotometer. For the absorption coefficient, solutions with concentrations of 0.0016 mg/mL in spectroscopic grade chloroform were analyzed. A Perkin–Elmer LS-50 spectrofluorimeter was used for the fluorescence spectra. Fluorescence quantum yields (ϕ) were calculated according to the methodology reported in Ref. 23, using a 1 N quinine sulfate solution in H_2SO_4 as the standard. The excitation wavelength for the dendrimers of first and second generation was 310 nm, 292 nm, and 305 nm, respectively. Briefly, solutions with absorbance at the excitation wavelength <0.1 mg/ml were prepared and their absorption and fluorescence spectra recorded. The values of the absorbance at the excitation wavelength and of the fluorescence integrated were introduced in the following formula:

$$\phi = \phi_{st}\frac{A_{st}F_s}{A_sF_{st}}\left(\frac{n_s}{n_{st}}\right)^2$$

where A_{st} and A_s are the absorbance values at the excitation wavelength for the standard and sample solution; F_{st} and F_s are the fluorescence integrated areas for the standard and sample solutions, while n_{st} and n_s are the corresponding refractive indexes. F_{st} is the known fluorescence quantum yield of the standard. Thin films were prepared from concentrated (10 mg/mL) chloroform solutions by spin-coating with a Clay-Adams equipment at around 3,000 rpm. The morphological characterization by AFM was realized with a Digital Instruments Atomic Dimension 3100 in tapping mode and at a scanning rate of 0.4–0.5 Hz. The tip was a TESP Veeco Probe with maximum ratio of curvature of 15 nm. The roughness of the surface topography (Rq) is given by the root mean square average (rms) of height deviation and is taken from the mean data plane, and expressed as: $Rq=[1/N\sum(Z_i)2]1/2$, where Z_i is the current Z value, and N is the number of points within the box. The thickness of the layers was obtained by profilometry by using a Dektak Stylus with a 12.5 mm tip and an applied force of 5 mg. The absorption coefficient in film (ε, nm^{-1}) was calculated by introducing the value of the thickness found by profilometry in a modified Lambert–Beer law $A=\varepsilon t$, where A is the absorbance and t is the thickness in nm. The optical band gap was obtained from the onset of the low energy absorption in the UV–vis spectra; the wavelength corresponding to the intersection of the tangent on the low energetic edge of the absorption spectrum with the abscissa, then is converted in energy applying the Planck equation.[24] For the determination of the photoluminescence quantum yield of films (η), the integrating sphere methodology reported by Friend at al. is usually performed for thin films of conjugated polymers.[25] The experimental set-up consists of an sphere, which has its inner surface coated with a diffusely reflecting barium sulfate, a spectrometer, and a laser that has a wavelength of 408 nm (in our case it resulted not to be proper for the molecules of the present study due to the fact that they present a very low absorption at this wavelength). As the excitation is very low, the emission spectrum is practically undetectable. For this reason, an indirect estimation of η was obtained by adapting the methodology for the determination of the fluorescence quantum yield of solutions previously described. In this case, the standard was a sample of a phenylene ethynylene film for which its η value was determined by integration

sphere method. The fluorescence spectra of the resorcinarene-dendrimer films and of the standard were recorded. The corresponding integrated areas under the absorption and emission spectra were calculated and inserted in the equation: $\eta = (A_{st}F_s)/(A_sF_{st})$ where A_{st} and A_s are the integrated areas under the absorption spectra of the standard and sample, respectively, while F_{st} and F_s are the corresponding integrated areas under the fluorescence spectra. All samples were excited under the same conditions. The electrochemical properties were obtained by cyclic voltammetry on a potentiostat/galvanostat ACM Gill AC. The reference electrode was a calomel electrode Accumet and the electrolyte was a 0.1 M CH_3CN (ACN) solution of Bu_4NPF_6. The experiments were carried out under nitrogen atmosphere with a scanning rate of 50 mV/s. The working electrode was a film of the material deposited on ITO (Aldrich, 15–25 Ω/cm^2) by spin-coating. The electrochemically reduced–oxidized films were removed from the cell, dried with nitrogen, and immediately recorded their UV–vis spectra. With regard to the energy level of the ferrocene–ferrocenium par reference that is of 4.8 eV below vacuum, one can calculate the orbital energies HOMO and LUMO from the oxidation (E_{ox}) and reduction (E_{red}) potentials with the formulas: HOMO (eV)$=-(E_{ox}+4.8)$, and LUMO (eV)$=-e(E_{red}+4.8)$[26] and therefore the electrochemical energy gap by E_g=LUMO−HOMO.

4.2. Synthesis of dendrons

A mixture of **1** or **6** (38 mmol), **2** (18.9 mmol), $Pd(OAc)_2$ (1.3 mmol), and tri-*o*-tolylphosphine POT (3.28 mmol) in Et_3N–DMF 1:5 (120 mL) was stirred under N_2 at 120 °C for 24 h. After cooling, the resulting mixture was filtered and the solvents evaporated. The crude product was purified by column chromatography (SiO_2, hexane).

4.2.1. (E) 3,5-Distyrylbenzaldehyde **3**

Yield 3.5 g (60%), white powder, mp 125–127 °C, UV CH_2Cl_2 (nm): 242, 311. IR (KBr, cm^{-1}): 3443, 3025, 2809, 2738, 1695 (C═O), 1590, 1449, 1143, 966, 884, 743, 694, 528. ^{1}H NMR (300 MHz, $CDCl_3$) δ_H (ppm): 7.13 (d, 2H, CH═, *J*=16.5 Hz), 7.23 (d, 2H, CH═, *J*=16.5 Hz), 7.27–7.45 (m, 4H, Ar), 7.35 (t, 2H, Ar, *J*=1.6 Hz), 7.54–7.60 (m, 4H, Ar), 7.87 (t, 2H, Ar, *J*=2.0 Hz), 7.92 (s, 1H, Ar), 10.09 (s, 1H, HC═O). ^{13}C NMR (75 MHz, $CDCl_3$) δ_C (ppm): 126.2 (CH═), 126.7 (Ar), 127.0 (CH═), 128.2 (Ar), 128.8 (Ar), 130.2 (Ar), 130.7 (Ar), 136.6 (Ar_{ipso}), 137.2 (Ar_{ipso}), 138.7 (Ar), 192.2 (C═O). MS EI$^+$ (*m*/*z*): 310. Anal. Calcd for $C_{23}H_{18}O$: C 89.00, H 5.85%. Found: C 89.10, H 5.86%.

4.2.2. 3,5-Bis((E)-3,5-di(E)-styrylstyryl)benzaldehyde **7**

Yield 9.5 g (70%), white powder, mp 131–133 °C, UV $CHCl_3$ (nm): 242.5, 316.5. IR (KBr, cm^{-1}): 3653, 3380, 3078, 3055, 3025, 2958, 2924, 2852, 2730, 1943, 1876, 1798, 1695 (C═O), 1635, 1591, 1493, 1450, 1383, 1280, 1178, 1137, 1080, 1029, 959, 876, 831, 805, 749, 719, 691, 567, 533, 491 ^{1}H NMR (300 MHz, $CDCl_3$) δ_H (ppm): 7.17 (d, 8H, CH═, *J*=16.2 Hz), 7.24 (d, 4H, CH═, *J*=16.5 Hz), 7.29–7.32 (m, 4H, Ar), 7.37–7.42 (m, 8H, Ar), 7.56–7.61 (m, 8H, Ar), 7.95 (t, 2H, Ar, *J*=1.5 Hz), 7.97 (s, 6H, Ar), 7.98 (s, 1H, Ar), 10.11 (s, 1H, HC═O). ^{13}C NMR (75 MHz, $CDCl_3$) δ_C (ppm): 124.0 (Ar), 124.5 (Ar), 126.6 (CH═), 127.5 (Ar), 127.8 (Ar), 128. 1 (Ar), 128.7 (Ar), 129.5 (Ar), 130.2 (Ar), 130.4 (Ar), 137.1 (Ar_{ipso}), 137.4 (Ar_{ipso}), 138.2 (Ar_{ipso}), 138.6 (Ar_{ipso}), 192.1 (C═O). MS FAB$^+$ (*m*/*z*): 718. Anal. Calcd for $C_{55}H_{42}O$: C 91.99, H 5.89%. Found: C 91.97, H 5.76%.

Lithium aluminum hydride (97%, 15.2 mmol) was dissolved in 50 mL of dry THF. To this solution, **3** or **7** (6.4 mmol) dissolved in 15 mL of dry THF were added dropwise using an addition funnel. The reaction was carried out at 0 °C for 4 h. After this time, 10 mL of water was added and the reaction mixture was filtered in Celite®. The solvent was evaporated and the residue was dissolved in dichloromethane. The resulting solution was dried with sodium sulfate, filtered, and the product was vacuum dried, and purified by column chromatography (Al_2O_3, hexane).

4.2.3. (E)-3,5-(Distyrylphenyl) methanol **4**

Yield 1.8 g (90%), white powder, mp 123–125 °C, UV CH_2Cl_2 (nm): 241, 302. IR (KBr, cm^{-1}): 3370, 3025, 2883, 1595, 1493, 1449, 1029, 961, 750, 693. ^{1}H NMR (300 MHz, $CDCl_3$) δ_H (ppm): 4.75 (s, 2H, CH_2), 5.18 (s, 1H, OH), 7.15 (s, 2H, CH═), 7.16 (s, 2H, CH═), 7.23–7.44 (m, 10H, Ar), 7.51 (d, 2H, Ar, *J*=1.5 Hz), 7.55 (t, 1H, Ar, *J*=1.5 Hz). ^{13}C NMR (75 MHz, $CDCl_3$) δ_C (ppm): 65.2 (CH_2–OH), 124.0 (Ar), 124.2 (Ar), 126.5 (Ar), 127.7 (CH═), 128.1 (CH═), 128.7 (Ar), 129.2 (Ar), 137.1 (Ar_{ipso}), 138.0 (Ar_{ipso}), 141.6 (Ar). MS EI$^+$ (*m*/*z*): 312. Anal. Calcd for $C_{23}H_{20}O$: C 88.46, H 6.41%. Found: C 88.49, H 6.38%.

4.2.4. (3,5-Bis((E)-3,5-di(E)-styrylstyryl)phenyl)methanol **8**

Yield 4.1 g (90%), white powder, mp 148–150 °C, UV CH_2Cl_2 (nm): 232, 315. IR (KBr, cm^{-1}): 3386, 3054, 3025, 2956, 2925, 2866, 1632, 1591, 1492, 1448, 1378, 1336, 1301, 1242, 1208, 1157, 1067, 1028, 958, 876, 834, 748, 691, 574, 532, 491. ^{1}H NMR (300 MHz, $CDCl_3$) δ_H (ppm): 4.70 (s, 1H, OH), 4.78 (s, 2H, CH_2), 7.15 (d, 4H, CH═, *J*=16.2 Hz), 7.22 (d, 8H, CH═, *J*=16.8 Hz), 7.26–7.31 (m, 4H, Ar), 7.36–7.41 (m, 8H, Ar), 7.49–7.55 (m, 8H, Ar), 7.56–7.59 (m, 8H, Ar), 7.64 (t, 1H, Ar, *J*=1.5 Hz). ^{13}C NMR (75 MHz, $CDCl_3$) δ_C (ppm): 65.0 (CH_2–OH), 123.9 (Ar), 124.1 (Ar), 126.5 (CH═), 127.7 (Ar), 128.3 (Ar), 128.7 (Ar), 128.9 (Ar), 129.2 (Ar), 137.2 (Ar), 137.8 (Ar_{ipso}), 137.9 (Ar_{ipso}), 138.0 (Ar_{ipso}), 141.8 (Ar_{ipso}). MS FAB$^+$ (*m*/*z*): 720. Anal. Calcd for $C_{55}H_{44}O$: C 91.63, H 6.15%. Found: C 91.47, H 6.18%.

Compound **4** or **8** (14.0 mmol), pyridine (1 mL, 14.0 mmol) and 1.45 mL (14.0 mmol) of $SOCl_2$ were dissolved in 100 mL of dry CH_2Cl_2, then this mixture was cooled to −10 °C. The reaction was carried out under nitrogen atmosphere in ice bath for 7 h. After this period, the solvent was evaporated and the resulting oil was dry supported and purified in a silica gel (60–240 pore size) column using a mixture of hexane–dichloromethane 2:1 as eluent.

4.2.5. (E)-1-(Chloromethyl)-3,5-distyrylbenzene **5**

Yield 4.1 g (90%), yellow-brown powder, mp 106–108 °C, UV $CHCl_3$ (nm): 242, 302. IR (KBr, cm^{-1}): 3026, 2924, 2953, 1596, 1493, 1450, 1261, 1155, 960, 750, 691. ^{1}H NMR (300 MHz, $CDCl_3$) δ_H (ppm): 4.63 (s, 2H, CH_2–Cl), 7.13 (d, 2H, CH═, *J*=16.4 Hz), 7.15 (d, 2H, CH═, *J*=16.6 Hz), 7.23–7.52 (m, 10H, Ar), 7.55 (t, 2H, Ar, *J*=2.5 Hz), 7.58 (t, 1H, Ar, *J*=1.5 Hz). ^{13}C NMR (75 MHz, $CDCl_3$) δ_C (ppm): 46.1 (CH_2–Cl), 124.7 (Ar), 125.6 (Ar), 126.5 (Ar), 127.8 (CH═), 129.6 (Ar), 136.9 (Ar_{ipso}), 138.1 (Ar_{ipso}), 138.2 (Ar). MS EI$^+$ (*m*/*z*): 330. Anal. Calcd for $C_{23}H_{19}Cl$: C 83.50, H 5.79%. Found: C 83.56, H 5.78%.

4.2.6. 5,5′-(1E,1′E)-2,2′-(5-(Chloromethyl)-1,3-phenylene)-bis(ethene-2,1-diyl)bis(1,3-di(E)-styrylbenzene) **9**

Yield 9.3 g (90%), yellow-brown powder, mp 156–158 °C, UV $CHCl_3$ (nm): 232, 316. IR (KBr, cm^{-1}): 3413, 3056, 3025, 2957, 2869, 1634, 1592, 1538, 1489, 1449, 1331, 1255, 1204, 1160, 1071, 958, 881, 834, 749, 690, 608, 564, 533, 491, 440. ^{1}H NMR (300 MHz, $CDCl_3$) δ_H (ppm): 4.66 (s, 2H, CH_2), 7.15 (d, 4H, CH═, *J*=16.4 Hz), 7.23 (d, 8H, CH═, *J*=16.2 Hz), 7.29 (s, 4H, Ar), 7.31–7.50 (m, 16H, Ar), 7.55–7.58 (m, 8H, Ar), 7.68 (br, 1H, Ar). ^{13}C NMR (75 MHz, $CDCl_3$) δ_C (ppm): 46.3 (CH_2), 123.9 (Ar), 124.3 (Ar), 124.8 (Ar), 125.9 (Ar), 126.5 (CH═), 127.2 (Ar), 127.8 (Ar), 128.2 (Ar), 128.4 (Ar), 128.7 (Ar), 129.4 (Ar), 137.1 (Ar), 137.7 (Ar), 138.1 (Ar), 138.3 (Ar_{ipso}), 138.5 (Ar_{ipso}), 141.3 (Ar_{ipso}), 145.6 (Ar_{ipso}). MS FAB$^+$ (*m*/*z*): 738. Anal. Calcd for $C_{55}H_{43}Cl$: C 89.34, H 5.86, Cl 4.79%. Found: C 89.32, H 5.76%.

Compound **3** (16.1 mmol) dissolved in dry THF (10 mL) was added to a mixture of methyl triphenylphosphine (16.1 mmol) in dry THF (100 mL) and *n*-buthyl lithium 2.5 M in hexanes (16.1 mmol) at 0 °C in N_2 atmosphere. The mixture was stirred for

24 h, then water was added (300 mL). The organic phase was evaporated to dryness and purified by column chromatography using hexane–ethyl acetate 4:1.

4.2.7. 1,3-Di(E)-styryl-5-vinylbenzene ***6***

Yield 4.6 g (92%), yellow-brown powder, mp 108–110 °C, UV $CHCl_3$ (nm): 312. IR (KBr, cm^{-1}): 3080, 3027, 2979, 2959, 2924, 2853, 1954, 1880, 1804, 1665, 1628, 1590, 1492, 1449, 1407, 1384, 1329, 1301, 1264, 1241, 1178, 1156, 1072, 1053, 1025, 984, 964, 913, 882, 835, 753, 693, 668, 585, 553, 533, 511, 484, 447. ^{1}H NMR (300 MHz, $CDCl_3$) δ_H (ppm): 5.32 (d, 1H, CH_2=, J=11.0 Hz), 5.84 (d, 1H, CH=, J=17.6 Hz), 6.77 (q, 1H, CH=), 7.15 (s, 2H, CH=), 7.16 (s, 2H, CH=), 7.23–7.46 (m, 10H, Ar), 7.52 (q, 2H, Ar), 7.56 (t, 1H, Ar, J=1.6 Hz). ^{13}C NMR (75 MHz, $CDCl_3$) δ_C (ppm): 114.5 (CH=), 123.6 (Ar), 122.1 (Ar), 126.5 (Ar), 127.7 (CH=), 128.3 (Ar), 128.7 (Ar), 129.2 (Ar), 136.6 (CH=), 137.2 (Ar_{ipso}), 137.9 (Ar_{ipso}), 138.2 (Ar_{ipso}). MS EI^+ (m/z): 308. Anal. Calcd for $C_{24}H_{20}O$: C 93.46, H 6.54%. Found: 93.44, H 6.44%.

The resorcinarenes were obtained in agreement with Ref. 8.

4.3. Synthesis of dendrimers

A mixture of the respective dendron **5** or **9** (1 mmol), potassium carbonate (21.2 mmol), and 18-crown-6 (0.56 g, 2.12 mmol) in dry acetone (80 mL) was heated to reflux and stirred vigorously in nitrogen atmosphere for 20 min. Compounds **10**–**12** (0.125 mmol) dissolved in dry acetone (40 mL) were added dropwise and the reaction was continued for 7 days. The mixture was cooled and the precipitate was filtered. The filtrate was evaporated to dryness under reduced pressure. The residue dissolved in diethyl ether was washed with an aqueous solution of 5% Na_2CO_3 (three times). The organic layer was dried and evaporated to dryness and the dendrimers were purified using the following procedure: the dendrimer was dissolved in CH_2Cl_2, then methanol was added producing precipitation of the dendrimer back. This procedure was repeated three times.

4.3.1. Dendrimer ***16***

Yield 0.37 g (91%), brown-red powder, mp >300 °C, UV–vis CH_2Cl_2 (nm): 241.5, 301.5. IR (KBr, cm^{-1}): 3429, 3025, 2925, 2861, 1943, 1798, 1597, 1494, 1452, 1376, 1294, 1180, 1105, 959, 749, 692, 534. ^{1}H NMR (300 MHz, $CDCl_3$) δ_H (ppm): 2.38 (br, 8H, CH_2), 2.77 (br, 8H, CH_2), 4.75 (m, 16H, CH_2–O), 4.78 (t, 4H, CH, J=7.0 Hz), 6.64 (s, 4H, Ar), 6.79 (d, 16H, CH=, J=16.2 Hz), 6.89 (d, 16H, CH=, J=16.2 Hz), 6.99 (s, 4H, Ar), 7.14–7.52 (m, 124H, Ar). ^{13}C NMR (75 MHz, $CDCl_3$) δ_C (ppm): 35.0 (CH), 36.3 (CH_2), 37.1 (CH_2), 70.0 (CH_2–O), 70.8 (CH_2–O), 123.5 (Ar), 124.7 (Ar), 125.3 (Ar), 126.5 (CH=), 127.0 (Ar), 127.5 (Ar), 128.1 (Ar), 128.2 (Ar), 128.6 (Ar), 128.8 (Ar), 129.2 (Ar), 137.0 (Ar_{ipso}), 137.4 (Ar_{ipso}), 137.9 (Ar), 142.5 (Ar_{ipso}), 155.2 (Ar–O). ES MS (m/z): 3260. Anal. Calcd for $C_{244}H_{200}O_8$: C 89.89, H 6.18%. Found: C 89.90, H 6.17%.

4.3.2. Dendrimer ***17***

Yield 0.35 g (91%), brown powder, mp >300 °C, UV–vis CH_2Cl_2 (nm): 242.5, 302, 391. IR (KBr, cm^{-1}): 3430, 3026, 2924, 2853, 1780, 1703, 1596, 1494, 1456, 1173, 1107, 961, 750, 694. ^{1}H NMR (300 MHz, $CDCl_3$) δ_H (ppm): 0.68 (t, 12H, CH_3, J=4.5 Hz), 1.23 (br, 16H, CH_2), 2.02 (br, 16H, CH_2), 4.63–4.87 (m, 16H, CH_2–O), 4.93 (m, 4H, CH), 6.65 (s, 4H, Ar), 6.80 (d, 16H, CH=, J=16.2 Hz), 6.89 (d, 16H, CH=, J=16.1 Hz), 6.96 (s, 4H, Ar), 7.15–7.5 (br, 104H, Ar). ^{13}C NMR (75 MHz, $CDCl_3$) δ_C (ppm): 14.0 (CH_3), 22.7 (CH_2), 32.3 (CH_2), 34.6 (CH), 69.9 (CH_2–O), 123.5 (Ar), 124.0 (Ar), 124.7 (Ar), 126.5 (Ar), 127.5 (CH=), 128.2 (Ar), 128.5 (Ar), 137.1 (Ar_{ipso}), 137.4 (Ar_{ipso}), 138.0 (Ar_{ipso}), 155.1 (Ar–O). ES MS (m/z): 3121. Anal. Calcd for $C_{232}H_{208}O_8$: C 89.19, H 6.71%. Found: C 89.20, H 6.71%.

4.3.3. Dendrimer ***18***

Yield 0.36 g (85%), brown powder, mp >300 °C, UV–vis CH_2Cl_2 (nm): 242.5, 301.5. IR (KBr, cm^{-1}): 3446, 3055, 3025, 2860, 1623, 1596, 1495, 1453, 1400, 1279, 1180, 1110, 1020, 959, 832, 749, 692. ^{1}H NMR (300 MHz, $CDCl_3$) δ_H (ppm): 0.87 (br, 12H, CH_3), 1.23 (br, 56H, CH_2), 1.68 (s, 8H, CH_2), 2.07 (m, 16H, CH_2), 4.76–5.25 (m, 16H, CH_2–O), 4.72 (s, 4H, CH), 6.42 (br, 4H, Ar), 7.05 (d, 16H, CH=, J=16.2 Hz), 7.13 (br, 4H, Ar), 7.14 (d, 16H, CH=, J=16.5 Hz), 7.27–7.61 (m, 104H, Ar). ^{13}C NMR (75 MHz, $CDCl_3$) δ_C (ppm): 14.0 (CH_3), 22.6 (CH_2), 29.3 (CH_2), 29.7 (CH_2), 31.9 (CH), 70.0 (CH_2–O), 112.0 (Ar), 118.0 (Ar), 124.3 (Ar), 126.5 (CH=), 127.5 (Ar), 127.7 (Ar), 128.0 (Ar), 128.6 (Ar), 130.2 (Ar), 136.8 (Ar_{ipso}), 137.1 (Ar_{ipso}), 138.1 (Ar), 138.8 (Ar_{ipso}), 155.3 (Ar–O). ES MS (m/z): 3458. Anal. Calcd for $C_{256}H_{256}O_8$: C 88.85, H 7.46. Found: C 88.85, H 7.44%.

4.3.4. Dendrimer ***19***

Yield 0.52 g (65%), brown powder, mp >300 °C, UV–vis CH_2Cl_2 (nm): 217, 231, 315, 564. IR (KBr, cm^{-1}): 3431, 3055, 3025, 2969, 2930, 1701, 1627, 1591, 1492, 1449, 1359, 1329, 1295, 1253, 1214, 1176, 1105, 1074, 1025, 958, 909, 881, 836, 782, 748, 692, 532, 492. ^{1}H NMR (300 MHz, $CDCl_3$) δ_H (ppm): 2.15 (br, 8H, CH_2), 2.60 (br, 8H, CH_2), 3.36–3.76 (m, 16H, CH_2–O), 4.53 (br, 4H, CH), 6.25 (br, 4H, Ar), 7.00 (br, 4H, Ar), 7.15 (d, 96H, CH=, J=14.7 Hz), 7.21–7.53 (m, 244H, Ar), 7.67 (br, 8H, Ar). ^{13}C NMR (75 MHz, $CDCl_3$) δ_C (ppm): 29.2 (CH_2), 31.6 (CH_2), 35.2 (CH), 69.4 (CH_2–O), 69.8 (CH_2–O), 123.9 (Ar), 126.5 (CH=), 127.7 (Ar), 128.3 (Ar), 128.7 (Ar), 129.2 (Ar), 137.1 (Ar), 137.6 (Ar_{ipso}), 137.8 (Ar_{ipso}), 138.0 (Ar_{ipso}), 138.5 (Ar_{ipso}), 155.23 (Ar–O). ES MS (m/z): 6523. Anal. Calcd for $C_{500}H_{392}O_8$: C 91.99, H 6.05%. Found: C 91.85, H 6.14%.

4.3.5. Dendrimer ***20***

Yield 0.48 g (60%), brown powder, mp >300 °C, UV–vis CH_2Cl_2 (nm): 231, 315, 557. IR (KBr, cm^{-1}): 3412, 3053, 3024, 2921, 2863, 1630, 1591, 1490, 1448, 1401, 1353, 1284, 1249, 1174, 1107, 1024, 958, 882, 837, 748, 692, 532, 490. ^{1}H NMR (300 MHz, $CDCl_3$) δ_H (ppm): 0.89 (br, 12H, CH_3), 1.25 (br, 16H, CH_2), 2.17 (br, 16H, CH_2), 3.50 (br, 16H, CH_2–O), 4.35 (br, 4H, CH), 6.19 (br, 4H, Ar), 7.18 (s, 20H, Ar), 7.22 (d, 96H, CH=, J=14.4 Hz), 7.29–7.55 (m, 216H, Ar). ^{13}C NMR (75 MHz, $CDCl_3$) δ_C (ppm): 14.7 (CH_3), 22.9 (CH_2), 29.2 (CH_2), 32.4 (CH), 69.9 (CH_2–O), 126.5 (CH=), 127.7 (Ar), 128.7 (Ar), 128.8 (Ar), 129.2 (Ar), 137.1 (Ar_{ipso}), 137.4 (Ar_{ipso}), 137.8 (Ar_{ipso}), 138.0 (Ar_{ipso}), 155.1 (Ar–O). ES MS (m/z): 6387.09. Anal. Calcd for $C_{488}H_{400}O_8$: C 91.69, H 6.31%. Found: C 91.59, H 6.40%.

4.3.6. Dendrimer ***21***

Yield 0.58 g (70%), brown powder, mp >300 °C, UV–vis CH_2Cl_2 (nm): 231, 315, 544. IR (KBr, cm^{-1}): 3376, 3079, 3056, 3025, 2923, 2853, 1655, 1591, 1489, 1445, 1379, 1254, 1164, 1107, 1072, 1022, 958, 881, 839, 783, 747, 691, 532, 491. ^{1}H NMR (300 MHz, $CDCl_3$) δ_H (ppm): 0.87 (br, 12H, CH_3), 1.25 (br, 64H, CH_2), 2.16 (m, 16H, CH_2), 3.44 (br, 16H, CH_2–O), 4.63 (s, 4H, CH), 7.18 (br, 40H, Ar), 7.24 (br, 96H, CH=), 7.28–7.57 (m, 208H, Ar). ^{13}C NMR (75 MHz, $CDCl_3$) δ_C (ppm): 14.1 (CH_3), 22.6(CH_2), 29.4 (CH_2), 29.7 (CH_2), 31.9 (CH), 69.9 (CH_2–O), 123.9 (Ar), 126.5 (CH=), 127.7 (Ar), 128.2 (Ar), 128.7 (Ar), 129.3 (Ar), 137.1 (Ar_{ipso}), 137.5 (Ar_{ipso}), 137.6 (Ar_{ipso}), 138.0 (Ar_{ipso}), 155.3 (Ar–O). ES MS (m/z): 6723.46. Anal. Calcd for $C_{512}H_{448}O_8$: C 91.39, H 6.71%. Found: C 91.37, H 6.81%.

Acknowledgements

This work was supported by the DGAPA (IN211408). We would also like to thank Nieves Z.S.M., Rios O.H., Velasco L., Huerta S.E., Patiño M.M.R., and Peña G.M.A. for technical assistance.

References and notes

1. Burroughes, J. H.; Bradley, D. D. C.; Brown, A. R.; Marks, R. N.; Mackay, K.; Friend, R. H.; Burns, P. L.; Holmes, A. B. *Nature* **1990**, *347*, 539.
2. Rothberg, L. J.; Yan, M.; Papadimitrakopoulos, F.; Galvin, M. E.; Kwock, E. W.; Miller, T. M. *Synth. Met.* **1996**, *80*, 41.
3. Reinhart, C. F. *The Future for Renewable Energy 2*; James & James Science: London, UK, 2002; pp 79–114.
4. Park, S. M. Electrochemistry of π-Conjugated Polymers. In *Conductive Polymers: Spectroscopy and Physical Properties*; Nalwa, H. S., Ed.; Handbook of Organic Conductive Molecules and Polymers; Willey-VCH: New York, NY, 1997; Vol. 3, p 429.
5. Joachim, C.; Gimzewski, J. K.; Aviram, A. *Nature* **2000**, *408*, 541.
6. Balzani, V.; Credi, A.; Raymo, F. M.; Stoddart, J. F. *Angew. Chem., Int. Ed.* **2000**, *39*, 3348.
7. Lehn, J. M. In *Supramolecular Chemistry, Concepts and Perspectives*; Gustav, F., Ed.; VCH: Weinheim, 1995; pp 39–51.
8. Holzwarth, J. F.; Whitesides, G. M. *Curr. Opin. Colloid Interface Sci.* **1996**, *1*, 61.
9. Dvornic, P. R.; Tomalia, D. A. *Macromol. Symp.* **1994**, *88*, 123.
10. Zeng, F.; Zimmerman, S. C. *Chem. Rev.* **1997**, *97*, 1861.
11. Tomalia, D. A.; Majoros, I. *Supramolecular Polymers*; Marcel Dekkers: New York, NY, 2000; p 359.
12. Newkome, G. R.; He, H.; Moorefield, C. N. *Chem. Rev.* **1999**, *99*, 1689.
13. Smith, D. K.; Diederich, F. *Top. Curr. Chem.* **2000**, *210*, 183.
14. Emrick, T.; Frechet, J. M. J. *Curr. Opin. Colloid Interface Sci.* **1999**, *4*, 15.
15. Bosman, A. W.; Janssen, H. M.; Meijer, E. W. *Chem. Rev.* **1999**, *99*, 1665.
16. (a) Lijanova, I. V.; Moggio, I.; Arias, E.; Vazquez-Garcia, R.; Martínez-García, M. *J. Nanosci. Nanotechnol.* **2007**, *7*, 3607. Consider that the quantum yield reported corresponds to the absolute and not % value; (b) Lijanova, I. V.; Reyes-Valderrama, M. I.; Maldonado, J. L.; Ramos-Ortiz, G.; Klimova, T.; Martínez-García, M. *Tetrahedron* **2008**, *64*, 4460.
17. Armaroli, N.; Accorsi, G.; Rio, Y.; Ceroni, P.; Vicinelli, V.; Welter, R.; Gu, T.; Saddik, M.; Hollerd, M.; Nierengarten, J.-F. *New J. Chem.* **2004**, *28*, 1627.
18. Gu, T.; Ceroni, P.; Marconi, G.; Armaroli, N.; Nierengarten, J.-F. *J. Org. Chem.* **2001**, *66*, 6432.
19. Devadoss, C.; Bharathi, P.; Moore, J. S. *J. Am. Chem. Soc.* **1996**, *118*, 9635.
20. Holzer, W.; Penzkofer, A.; Stockmann, R.; Meysel, H.; Liebegott, H.; Hörhold, H. H. *Polymer* **2001**, *42*, 3183.
21. Liu, H.; Wang, S.; Luo, Y.; Tang, W.; Yu, G.; Li, L.; Chen, C.; Liu, Y.; Xi, F. *J. Mater. Chem.* **2001**, *1*, 3063.
22. Wa Santos, L. F.; Gaffo, L.; De Carvalho, L. M.; Gonçalves, D.; Faria, R. M. *Mol. Cryst. Liq. Cryst.* **2002**, *374*, 469; (b) Zotti, G.; Zecchin, S.; Schiavon, G. *Macromolecules* **2001**, *34*, 3889; (c) Ferraris, J. P.; Elissa, M. M.; Brotherson, I. D.; Moxey, A. A.; Loveday, D. C. *J. Electroanal. Chem.* **1998**, *57*, 459.
23. Williams, A. T. R.; Winfield, S. A.; Miller, J. N. *Analyst* **1983**, *108*, 1067.
24. Colladet, K.; Fourier, S.; Cleij, T. J.; Lutsen, L.; Gelan, J.; Vanderzande, D.; Nguyen, L.; Neugebauer, H.; Sariciftci, S.; Aguirre, A.; Janssen, G.; Goovaerts, E. *Macromolecules* **2007**, *40*, 65.
25. De Mello, J. C.; Wittmann, H. F.; Friend, R. H. *Adv. Mater.* **1997**, *9*, 230.
26. (a) Jandke, M.; Strohriegl, P.; Berleb, S.; Werner, E.; Brütting, W. *Macromolecules* **1998**, *31*, 6434; (b) Schweitzer, B.; Bässler, H. *Synth. Met.* **2000**, *109*, 1.